Oral SARS-CoV-2 Inoculation Causes Nasal Viral Infection Leading to Olfactory Bulb Infection: an Experimental Study

Rumi Ueha (ruu1025@yahoo.co.jp)
the University of Tokyo
Toshihiro Ito
Nara Medical University
Ryutaro Furukawa
Nara Medical University
Masahiro Kitabatake
Nara Medical University
Noriko Ouji-Sageshima
Nara Medical University
Satoshi Ueha
Tokyo University of Science
Misaki Koyama
the University of Tokyo
Tsukasa Uranaka
the University of Tokyo
Kenji Kondo
the University of Tokyo
Tatsuya Yamasoba
the University of Tokyo

Research Article

Keywords: SARS-CoV-2, oral inoculation, olfactory dysfunction, olfactory epithelium, zone, olfactory bulb

Posted Date: January 27th, 2022

DOI: https://doi.org/10.21203/rs.3.rs-1204399/v1

Abstract

Severe acute respiratory syndrome coronavirus 2 (SARS-CoV-2) infections can cause long-lasting anosmia, but the impact of SARS-CoV-2 infection, which can spread to the nasal cavity via the oral route, on the olfactory receptor neuron (ORN) lineage and olfactory bulb (OB) remains undetermined. Using Syrian hamsters, we explored whether oral SARS-CoV-2 inoculation can lead to nasal viral infection, examined how SARS-CoV-2 affects the ORN lineage by site, and investigated whether SARS-CoV-2 infection can spread to the OB and induce inflammation. On post-inoculation day 7, SARS-CoV-2 presence was confirmed in the lateral area (OCAM-positive) but not the nasal septum of NQO1-positive and OCAM-positive areas. The virus was observed partially infiltrating the olfactory epithelium, and ORN progenitor cells, immature ORNs, and mature ORNs were fewer than in controls. The virus was found in the olfactory nerve bundles to the OB, suggesting the nasal cavity as a route for SARS-CoV-2 brain infection. We demonstrated that transoral SARS-CoV-2 infection can spread from the nasal cavity to the central nervous system and the possibility of central olfactory dysfunction due to SARS-CoV-2 infection. The virus was localized at the infection site and could damage all ORN-lineage cells.

Introduction

At the end of 2019, severe acute respiratory syndrome coronavirus 2 (SARS-CoV-2) was identified as the cause of a cluster of pneumonia cases in China, which rapidly spread, resulting in a global pandemic [1]. SARS-CoV-2 infection (coronavirus disease; COVID-19) is associated with upper respiratory tract symptoms such as nasal discharge and sore throat, spreading to the lower respiratory tract, resulting in pneumonia, which in severe cases may require artificial respiration management [1,2].

The characteristic symptoms of SARS-CoV-2 infection (COVID-19) comprise sensory impairments such as olfactory and gustatory dysfunctions. Among these, olfactory dysfunction is seen in 20–85% of patients [3–5], and more patients present with anosmia (complete loss of the sense of smell) than with partial olfactory disturbance [6,7].

The coronavirus receptor proteins including angiotensin-converting enzyme 2 (ACE2) [8] and neuropilin-1 [9], as well as proteases such as transmembrane protease serine 2 (TMPRSS2) [8] and Furin [10], which assist the virus in entering tissues, are found in the upper respiratory tract, including the tongue, nasal cavity, and pharynx [11,12]. Therefore, the nasal and oral cavities are considered the major routes of SARS-CoV-2 infection. Although the mechanisms underlying olfactory dysfunction related to COVID-19 have been gradually elucidated through histological and genomic examinations [7,11–13] and imaging studies [14,15], it remains difficult to disentangle the involved mechanisms because of the heterogeneity of presentations [16]. Currently, the following mechanisms are being considered: 1) transient conductive olfactory dysfunction resulting from airway blockage due to local inflammation and edema of the nasal mucosa in the olfactory cleft and nasal passages; 2) temporary sensorineural olfactory dysfunction due to damage to supporting tissues such as the sustentacular cells, Bowman's gland, and microvillar cells, excluding

mature olfactory receptor cells (ORNs); 3) chronic or permanent sensorineural olfactory dysfunction due to damage to the ORNs; 4) central olfactory dysfunction due to SARS-CoV-2 infection of the olfactory bulb (OB) and olfactory cortex [16–18].

Several studies using tissue samples from SARS-CoV-2-infected hamsters and humans have been reported to elucidate the mechanism of olfactory dysfunction [17,19–22]. Mouse species have been evaluated with SARS-CoV-2, but most do not show severe clinical signs because of disparity between mouse and human ACE2 [23]. In contrast, the Syrian hamster ACE2 is highly homologous to human ACE2 and efficiently binds to the SARS-CoV-2 receptor binding domain; therefore, the Syrian hamster is recognized as a good small animal model for SARS-CoV-2 infection [23,24]. In Syrian hamsters, the olfactory epithelium (OE) is extensively disrupted in the first few days after SARS-CoV-2 infection, and the loss of microvilli becomes significant on days 2–7 [20,22]. The virus mainly infects the sustentacular and microvillar cells and not the ORNs in the OE [19,22]. Subsequently, immune cells are recruited and infiltrate the OE and lamina propria of the olfactory mucosa (OM) [19,21]. OE regeneration begins at approximately day 8 and is almost restored by day 21 in the nasal septum, while regeneration is insufficient in the lateral and dorsal regions [20]. This means that the regeneration process varies depending on the location in the nasal cavity. The ORNs are classified into four groups according to their zonal expression patterns, and odorant receptors are expressed by sensory neurons distributed within one of four circumscribed zones [25–27]. Of those, zone 1 is determined by co-localization with NQO1 expression and zones 2–4 are determined by OCAM expression [25–28]. However, the impacts of various viral infections on the ORNs, including ORN progenitor cells and immature ORNs, have not been well established, and especially, the effects of SARS-CoV-2 infection on each zone of the OE has not been verified. Additionally, the effects of SARS-CoV-2 infection on the OB, the center of olfaction, are poorly understood, although they can cause long-lasting and complete loss of smell [6,7]. It is imperative to uncover the routes of SARS-CoV-2 infection and transmission to prevent and develop treatments for this sensory disorder that reduces the quality of life.

Although it is unlikely that the nasal route is actually the only SARS-CoV-2 nasal infection route, the transnasal route of SARS-CoV-2 is often applied in experimental models to investigate olfactory disorders. It is conceivable that SARS-CoV-2 may also spread to the nasal cavity via the oral route, but this possibility has not been verified. Therefore, clarification is needed to determine whether oral infection can also transmit the virus to the OM and OB.

In this study, we first explored whether oral SARS-CoV-2 inoculation, not nasal administration, can lead to nasal viral infection using hamster models. Secondly, we examined how SARS-CoV-2 affects the OE, including ORN-related cells, by site. Third, we investigated whether SARS-CoV-2 infection can spill over to the OB and induce inflammation.

Methods

Animals

Six-week-old, male Syrian Golden hamsters (*Mesocricetus auratus*) were purchased from Japan SLC (Hamamatsu, Shizuoka, Japan) and maintained in a specific pathogen-free environment at the Animal Research Center of Nara Medical University. The animal experimental protocols were complied with the ARRIVE guidelines, and approved by The Animal Care and Use Committee at Nara Medical University (approval number, 12922). All procedures were performed in compliance with relevant guidelines on the Care and Use of Laboratory Animals, Nara Medical University and Animal Research and the Animal Care and Use Committee of the University of Tokyo.

Infection model preparation

The SARS-CoV-2 strain (JPN/TY/WK-521) was isolated and provided by the National Institute of Infectious Diseases, Japan. Virus culture was performed using VeroE6/TMPRSS2 cells (JCRB Cell Bank in Japan, JCRB1819). Hamsters were distributed into two groups. Before virus inoculation, they were anesthetized with an intraperitoneal injection of pentobarbital. In the infection group, 50 μL of virus solution diluted by saline (including 1.0×10^5 pfu of SARS-CoV-2) was administered into the mouth following the method of the previous paper [29]. In the control group, 50 μL of saline was administered. At 7 days after inoculation, the SARS-CoV-2-challenged hamsters were euthanized by intraperitoneal injection of 1.0 ml sodium pentobarbital (10mg/ml) followed by cardiac exsanguination. The noses and OBs were sampled for histopathological examination and the lungs for histopathological examination and quantitative polymerase chain reaction (qPCR). All experiments using SARS-CoV-2 were performed at the biosafety level 3 experimental facility of Nara Medical University, Japan.

RNA extractions and RT-qPCR

We verified the SARS-CoV-2 viral RNA in the lungs to confirm that each hamster was infected with SARS-CoV-2. Total RNA was isolated from the lung using NucleoSpin® RNA (Macherey-Nagel, Düren, Germany), then converted to cDNA using a High-Capacity cDNA Reverse Transcription Kit (Thermo Fisher Scientific, Waltham, MA, USA), according to the manufacturer's instructions. RT-qPCR analysis was performed using a StepOnePlus Real-Time PCR System (Thermo Fisher Scientific). The gene-specific primers and probes used were: *Gapdh* as endogenous control (TaqMan assay Cg04424038) and SARS-CoV-2 nucleocapsid gene (forward: 5'- AAATTTTGGGGACCAGGAAC -3', reverse: 5'- TGGCAGCTGTGTAGGTCAAC -3', the TaqMan probe: FAM-ATGTCGCGCATTGGCATGGA-BHQ). The expression levels of each gene were normalized to the level of *Gapdh* expression for each sample.

Tissue preparation

Immediately after tissue harvesting, the lungs and nasal tissues were gently irrigated and fixed in 4% paraformaldehyde for 14 days. Then, the tissue samples were decalcified, dehydrated in graded ethanol solutions, and embedded in paraffin. For histological analysis of the OM, coronal sections were obtained from all samples at the level of the anterior end of the OB [30–33]. Four-micrometer-thick paraffin sections were deparaffinized in xylene and rehydrated in ethanol before staining.

Histological analyses

Hematoxylin and eosin staining was performed to evaluate the overall tissue structure. For immunostaining, deparaffinized sections were treated with 3% hydrogen peroxide to block endogenous peroxidase activity, and then incubated in Blocking One solution (Nacalai Tesque, Kyoto, Japan) to block non-specific immunoglobulin binding. After antigen retrieval, the samples were incubated with primary antibodies, followed by secondary antibodies.

The primary antibodies used in this study are listed in Table 1. Anti-NQO1 and anti-OCAM antibodies were used to confirm the location of zone 1 or zones 2–4. Anti-SARS-CoV-2 nucleocapsid antibody was used to identify SARS-CoV-2. The following antibodies were used to evaluate ORN neurogenesis: sex-determining region Y-box 2 (SOX2), expressed by proliferating stem cells or progenitor cells in the basal layer of the OE; growth-associated protein 43 (GAP43), expressed by immature ORNs in the OE; olfactory marker protein (OMP), expressed by mature ORNs in the OE. Ki67 and cleaved caspase-3 (Cas3) were used as cellular markers for proliferation and for cell death, separately. To assess inflammatory cell infiltration, CD3 and MPO were used for detection of T cells and for polymorphonuclear neutrophils and macrophages, respectively [34,35]. Ionized calcium-binding adaptor molecule 1 (Iba1), a microglial marker, was applied as an indicator of the inflammatory response in the OB [36].

Table 1
The primary antibodies used in this study

Primary antibody	Source	Catalog No.	Host	Type	Dilution
OCAM	R&D Systems (Minneapolis, MN, USA)	AF778	Goat	polyclonal	1:200
NQO1	Abcam (Cambridge, UK),	ab34173	Rabbit	polyclonal	1:500
SARS-CoV-2 nucleocapsid	GeneTex(Irvine, CA, USA)	GTX135357	Rabbit	polyclonal	1:1000
SOX2	Abcam (Cambridge, UK),	ab92494	Rabbit	monoclonal	1:300
GAP43	Novus Biologicals (Centennial, CO, USA)	NB300-143B	Rabbit	polyclonal	1:1000
OMP	Wako (Tokyo, Japan)	019-22291	Goat	polyclonal	1:8000
CD3	Nichirei (Tokyo, Japan)	413601	Rabbit	monoclonal	1:300
MPO	Abcam (Cambridge, UK),	ab9535	Rabbit	polyclonal	1:150
PGP9.5	Dako (Carpinteria, CA, USA)	Z5116	Rabbit	polyclonal	1:1000
Ki67	Novus Biologicals (Centennial, CO, USA)	NB600-1252	Rabbit	monoclonal	1:200
Caspase-3	Cell Signaling (Tokyo, Japan)	9661	Rabbit	polyclonal	1:300
IBA1	Proteintech (Tokyo, Japan)	10904-1-AP	Rabbit	polyclonal	1:1000

To analyze the OE, coronal sections of the OE were divided into four areas along the zonal organization: the dorsal nasal septum (DS) area, ventral nasal septum (VS) area, dorsal lateral turbinate (DLT) area, and lateral turbinate (LT) area (Figure 1A). To analyze the OB, coronal sections of the OB-surrounding tissue were divided into three areas: the cribriform plate area, medial area, and lateral area.

Images were captured using a digital microscope camera (Keyence BZ-X700, Osaka, Japan) with 4×, 20×, and 40× objective lenses. OMP^+ ORNs, $SOX2^+$ ORN progenitors, $GAP43^+$ immature ORNs, and $Ki67^+$ cells in a 300-μm region of each area were counted in the right and left sides of each sample. The number of each cell type was quantitatively analyzed using sections with single or double immunostaining for each antigen and counterstaining with hematoxylin or DAPI.

Statistical analysis

Statistical comparisons between groups were performed with the Mann–Whitney U-test using GraphPad Prism software (version 6.7; GraphPad Software, Inc., San Diego, CA, USA, www.graphpad.com). qPCR

data were subjected to logarithmic transformation prior to analysis. Results with $P < 0.05$ were considered statistically significant.

Results

Oral SARS-CoV-2 inoculation induces nasal infection in a zone/site-dependent manner

To confirm that SARS-CoV-2 infection was established, we first examined the presence of the virus in the lungs with RT-qPCR and immunohistochemistry. The virus was identified histologically and with RT-qPCR in the lungs of SARS-CoV-2-infected hamsters on day 7 after oral inoculation, and SARS-CoV-2 infection was observed in all hamsters orally inoculated (Figure 1A, B). Next, we investigated the zone expression of the OM. In the OM of control hamsters, the DS area was NQO1 positive and all other areas (VS, DLT, LT) were OCAM positive (Figure 1C, D). Similarly, in SARS-CoV-2 hamsters, the OE could be divided into NQO1-positive and OCAM-positive regions (Figure 1E, F). Then, we examined the nasal cavity for the presence of SARS-CoV-2 through immunostaining on day 7 after oral virus inoculation. Although SARS-CoV-2 was not detected in the NS (NQO1-positive) and VS (OCAM-positive) areas of the nasal cavity of infected hamsters, the virus was extensively confirmed in the DLT and LT (OCAM-positive) areas. The virus was observed infiltrating a part of the OE and predominantly around OMP-negative cells in the OE (Figure 1G, H).

SARS-CoV-2 infection reduces the olfactory receptor neurons at various differentiation stages

We subsequently examined the effect of SARS-CoV-2 infection on the ORN lineage. The numbers of $SOX2^+$ ORN progenitor cells, $GAP43^+$ immature ORNs, and OMP^+ mature ORNs were lower in the infected group than in the control group on day 7 after SARS-CoV-2 infection in all four areas. In the control group, the middle layer of the OE was almost completely filled with OMP^+ ORNs, whereas in the SARS-CoV-2 infected group, OMP-negative cells were scattered in the middle layer of the OE to varying degrees, and these cells were negative for both GAP43 and SOX2 (Figure 2). $Ki67^+$ dividing cells were found in the most superficial layer of the OE in the DS and VS areas, but not in the strongly infected lateral regions (DLT and LT). Few apoptotic cells were found in the entire nasal cavity. Regarding inflammatory cell infiltration, some MPO^+ cells were found in the DLT and LT regions, where SARS-CoV-2 was found, but a few CD3 positive cells were present in the VS, LT, and MT regions. In brief, the DS region showed the least inflammatory cell infiltration on day 7 after SARS-CoV-2 infection (Figure 3).

SARS-CoV-2 can invade the olfactory bulb from the olfactory epithelium via the olfactory nerve

Last, we examined whether SARS-CoV-2 could enter the central nervous system through the nasal cavity. The olfactory nerve fibers, which transmit odor information from the ORNs, penetrate a small hole in the

cribriform plate of the ethmoid bone and reach the OB. In the SARS-CoV-2 infected group, the virus was found in the olfactory nerve on the nasal side and the olfactory nerve fiber layer on the OB side, suggesting that the nasal cavity is a route to brain infection in COVID-19. In addition, a small amount of SARS-CoV-2 was seen in the medial region of the OB (Figure 4). However, there was minor inflammatory cell infiltration in the OB, and only few MPO^+ and $CD3^+$ cells were observed in the lamina propria of the OM close to the cribriform plate. No obvious increase in $Iba1^+$ activated microglia was observed in the OB of the SARS-CoV-2 group (Figure 5).

Discussion

The present study showed that SARS-CoV-2 infection via the oral route can spread to the nasal cavity and OB in Syrian hamsters. SARS-CoV-2 was detected in the nasal cavity 7 days after oral SARS-CoV-2 inoculation, but the virus infection site was mainly on the lateral side of the nasal cavity. The numbers of ORN-associated cells were reduced in all lineages. SARS-CoV-2 was identified in the olfactory nerve bundles in the pathway from the OM to the OB.

Although the infection conditions in the nasal cavity may be different between the transnasal and transoral infection models of SARS-CoV-2, the virus oral inoculation model may show an infection situation more similar to the actual living environment than the virus nasal administration model. The findings that SARS-CoV-2 entering the host animals via the oral route not only infected the lower respiratory tract, but also the nasal tissues and induced degeneration of the OE, is an important message regarding infection countermeasures in daily life. By inhaling droplets from conversations during eating and drinking, or by eating something touched with SARS-CoV-2-contaminated hands, the virus is likely to adhere to the oral cavity and enter the body, resulting in olfactory dysfunction in some people. Therefore, individuals should thoroughly wash their hands before eating, be careful of splashing droplets during conversation while eating, and avoid sharing meals with others to prevent infection.

Regarding the localization of SARS-CoV-2 infection sites in the nasal cavity and differences in the OE damage depending on the site, a previous report showed that it is more likely for SARS-CoV-2 to be found in the lateral region where there is a greater degree of tissue damage [20], which is consistent with the present results. In addition, this is also analogous to the fact that the OE in the dorsolateral region is susceptible to damage via allergic inflammation [37]. Conversely, it has been reported that the NQO1-positive OE is more likely to be damaged by long-term exercise and caloric restriction [38]. Thus, it is suggested that the susceptibility of the OM to damage depends on the type of damage and the location of the OE.

Many studies have examined which OE cells are susceptible to infection by SARS-CoV-2, and it is now considered that the virus primarily infects the olfactory cilia and supporting cells but can also infect some basal ORN progenitors [9,19,21,22]. However, SARS-CoV-2 can also affect olfactory neurons, albeit slightly [21]. In the present validation, the numbers of all ORN-related cells, including ORN progenitors, immature ORNs, and mature ORNs, were reduced in each area of the OE compared to the control group, although

differences were observed in each area of the OE. Although the present study was limited to the analysis of day 7 after oral SARS-CoV-2 inoculation, and the temporal changes before and after the infection could not be confirmed, we discuss the following.

In the DS and VS areas where the virus could not be identified, the epithelial layer of the SARS-CoV-2 group was thinner than that of the control group. The numbers of basal cells, immature ORNs, and mature ORNs were reduced, and only the cells in the superficial layer of the OE were dividing, suggesting that the OE was damaged after virus infection and that it may have been in the regeneration stage at the time of examination. As $GAP43^+$ immature ORNs could not be identified and $Ki67^+$ cells were observed in the superficial layer, rather than in the basal layer, we speculate that the time point we verified in this study was the stage when the damaged sustentacular cells had first started to regenerate and that the basal cells ($SOX2^+$ ORN progenitors) and their differentiation process to $GAP43^+$ immature ORNs are suppressed by SARS-CoV-2 infection. Considering that inflammatory cell infiltration is not as abundant in the OM, it is presumed that the OE damage was induced by direct cell damage caused by the virus rather than by the effects of inflammatory cell infiltration. In the previously reported transnasal infection model of SARS-CoV-2, SARS-CoV-2 mainly infected the sustentacular cells, not the ORNs, and most of their cilia were lost early after infection [19,22]. It was also reported that SARS-CoV-2 could only be identified in the nasal septum of intranasal infected hamsters up to 3 days after infection [20], which is consistent with our results. In the nasal septum of this animal model, a large proportion of the OE was damaged within a few days after infection, followed by epithelial regeneration over time [20]. Although the temporal changes after infection in the oral SARS-CoV-2 inoculation model may differ from those in the transnasal infection model, we speculate that the DS and VS areas, where no SARS-CoV-2 was identified in this study, will regenerate their epithelial tissue.

In the DLT and LT areas where the virus was present, while sustentacular cells and basal ORN progenitors could be seen to some extent, immature ORNs could hardly be seen, and mature ORNs could only be sparsely seen. As several cells negative for SOX2, GAP43, and OMP were found in the middle layer of the OE, it is possible that SARS-CoV-2 impaired the function of mature ORNs and prevented normal ORN protein expression. Taken together, the possible effects of SARS-CoV-2 infection on the ORNs are as follows: (1) sustentacular cells cannot support the ORNs because of viral infection, resulting in difficulty in maintaining the epithelial morphology and reduced function of mature ORNs [9,19,21,22]; (2) SARS-CoV-2 directly infects the ONRs and reduces their function, although the percentage may be small [21]; and (3) SARS-CoV-2 may inhibit the maturation and differentiation of immature ORNs into mature ORNs.

The olfactory route is considered a potential means for SARS-CoV-2 to invade the central nervous system [39]. In this study, we found SARS-CoV-2 in the olfactory nerve bundle around the cribriform plate, indicating that the nasal cavity is an entry route for the virus to invade the central nervous system. In human studies, SARS-CoV-2 has been detected in the OB of autopsied cases [40,41]. Imaging studies have also shown hyperintensity of the OB on T2 fluid-attenuated inversion recovery magnetic resonance images [15,42] and a pattern of hypometabolism involving the olfactory system (orbitofrontal cortex and

olfactory and rectus gyri) on positron emission tomography of brain [43]. A study on rhesus monkeys reported that SARS-CoV-2 primarily invades the central nervous system via the OB [39]. In human angiotensin-converting enzyme 2 transgenic mice infected with SARS-CoV-2, viral RNA was detected throughout the OB, including in the olfactory nerve layer, 7 days after infection [44]. Approximately 10% of patients continued to experience olfactory dysfunction more than 6 months after SARS-CoV-2 infection [45,46], suggesting that the virus affected the central olfactory system, and the results of this study support the possibility of central olfactory dysfunction due to SARS-CoV-2 infection.

In conclusion, this study suggests that transoral SARS-CoV-2 infection may spread to the nasal cavity and then to the central nervous system through the olfactory route. To prevent SARS-CoV-2 infection in daily life, individuals should take adequate infection prevention measures and avoid performing activities associated with transoral infection.

Abbreviations

ACE2: angiotensin-converting enzyme 2

COVID-19: coronavirus disease

DLT: dorsal lateral turbinate

DS: dorsal nasal septum

GAP43: growth-associated protein 4

Iba1: ionized calcium-binding adaptor molecule 1

LT: lateral turbinate

OB: olfactory bulb

OE: olfactory epithelium

OM: olfactory mucosa

OMP: olfactory marker protein

ORN: olfactory receptor neuron

qPCR: quantitative polymerase chain reaction

SARS-CoV-2: severe acute respiratory syndrome coronavirus 2

SOX2: sex-determining region Y-box 2

TMPRSS2: transmembrane protease serine 2

VS: ventral nasal septum

Declarations

Acknowledgements

Not applicable.

Authors' contributions

R.U. developed the concept, designed and performed the experiments, analyzed the data, produced the figures, and wrote the initial draft of the manuscript. TI, RF, MK, and NOS prepared the animal models, performed some of the experiments, and analyzed the data. MK and TU performed some of the experiments and analyzed the data. KK and TY developed the concept and designed and critically revised the manuscript. All authors contributed to interpretation of the data and writing of the manuscript.

Competing interests

There are no competing interests.

Funding

This work was supported by JSPS KAKENHI Grant-in-Aid for Scientific Research (C) [grant number 19K09841], and MSD Life Science Foundation.

Availability of data and materials

The datasets used and/or analyzed during the current study are available from the corresponding author on reasonable request.

References

1. Wang, C., Horby, P. W., Hayden, F. G. & Gao, G. F. A novel coronavirus outbreak of global health concern. *Lancet* **395**, 470-473, doi:10.1016/S0140-6736(20)30185-9 (2020).
2. Jiang, S., Xia, S., Ying, T. & Lu, L. A novel coronavirus (2019-nCoV) causing pneumonia-associated respiratory syndrome. *Cellular & molecular immunology* **17**, 554, doi:10.1038/s41423-020-0372-4 (2020).
3. Han, A. Y., Mukdad, L., Long, J. L. & Lopez, I. A. Anosmia in COVID-19: Mechanisms and Significance. *Chemical senses*, doi:10.1093/chemse/bjaa040 (2020).
4. Costa, K. *et al.* Olfactory and taste disorders in COVID-19: a systematic review. *Brazilian journal of otorhinolaryngology* **86**, 781-792, doi:10.1016/j.bjorl.2020.05.008 (2020).

5. Ibekwe, T. S., Fasunla, A. J. & Orimadegun, A. E. Systematic Review and Meta-analysis of Smell and Taste Disorders in COVID-19. *OTO open* **4**, 2473974X20957975, doi:10.1177/2473974X20957975 (2020).
6. Saussez, S., Lechien, J. R. & Hopkins, C. Anosmia: an evolution of our understanding of its importance in COVID-19 and what questions remain to be answered. *European archives of oto-rhino-laryngology : official journal of the European Federation of Oto-Rhino-Laryngological Societies* **278**, 2187-2191, doi:10.1007/s00405-020-06285-0 (2021).
7. Butowt, R. & von Bartheld, C. S. Anosmia in COVID-19: Underlying Mechanisms and Assessment of an Olfactory Route to Brain Infection. *The Neuroscientist : a review journal bringing neurobiology, neurology and psychiatry* **27**, 582-603, doi:10.1177/1073858420956905 (2021).
8. Hoffmann, M. *et al.* SARS-CoV-2 Cell Entry Depends on ACE2 and TMPRSS2 and Is Blocked by a Clinically Proven Protease Inhibitor. *Cell* **181**, 271-280 e278, doi:10.1016/j.cell.2020.02.052 (2020).
9. Cantuti-Castelvetri, L. *et al.* Neuropilin-1 facilitates SARS-CoV-2 cell entry and infectivity. *Science* **370**, 856-860, doi:10.1126/science.abd2985 (2020).
10. Walls, A. C. *et al.* Structure, Function, and Antigenicity of the SARS-CoV-2 Spike Glycoprotein. *Cell* **181**, 281-292 e286, doi:10.1016/j.cell.2020.02.058 (2020).
11. Sato, T. *et al.* Expression of ACE2 and TMPRSS2 Proteins in the Upper and Lower Aerodigestive Tracts of Rats: Implications on COVID 19 Infections. *The Laryngoscope* **131**, E932-E939, doi:10.1002/lary.29132 (2021).
12. Ueha, R. *et al.* ACE2, TMPRSS2, and Furin expression in the nose and olfactory bulb in mice and humans. *Rhinology* **59**, 105-109, doi:10.4193/Rhin20.324 (2021).
13. Singh, M., Bansal, V. & Feschotte, C. A Single-Cell RNA Expression Map of Human Coronavirus Entry Factors. *Cell reports* **32**, 108175, doi:10.1016/j.celrep.2020.108175 (2020).
14. Naeini, A. S. *et al.* Paranasal sinuses computed tomography findings in anosmia of COVID-19. *American journal of otolaryngology* **41**, 102636, doi:10.1016/j.amjoto.2020.102636 (2020).
15. Keshavarz, P. *et al.* A Systematic Review of Imaging Studies in Olfactory Dysfunction Secondary to COVID-19. *Academic radiology* **28**, 1530-1540, doi:10.1016/j.acra.2021.08.010 (2021).
16. Xydakis, M. S. *et al.* Post-viral effects of COVID-19 in the olfactory system and their implications. *The Lancet. Neurology* **20**, 753-761, doi:10.1016/S1474-4422(21)00182-4 (2021).
17. Zhang, A. J. *et al.* Severe Acute Respiratory Syndrome Coronavirus 2 Infects and Damages the Mature and Immature Olfactory Sensory Neurons of Hamsters. *Clinical infectious diseases : an official publication of the Infectious Diseases Society of America* **73**, e503-e512, doi:10.1093/cid/ciaa995 (2021).
18. Ye, Q. *et al.* SARS-CoV-2 infection in the mouse olfactory system. *Cell discovery* **7**, 49, doi:10.1038/s41421-021-00290-1 (2021).
19. Bryche, B. *et al.* Massive transient damage of the olfactory epithelium associated with infection of sustentacular cells by SARS-CoV-2 in golden Syrian hamsters. *Brain, behavior, and immunity* **89**, 579-586, doi:10.1016/j.bbi.2020.06.032 (2020).

20. Urata, S. *et al.* Regeneration Profiles of Olfactory Epithelium after SARS-CoV-2 Infection in Golden Syrian Hamsters. *ACS chemical neuroscience* **12**, 589-595, doi:10.1021/acschemneuro.0c00649 (2021).
21. de Melo, G. D. *et al.* COVID-19-related anosmia is associated with viral persistence and inflammation in human olfactory epithelium and brain infection in hamsters. *Science translational medicine* **13**, doi:10.1126/scitranslmed.abf8396 (2021).
22. Seo, J. S. *et al.* The Microvillar and Solitary Chemosensory Cells as the Novel Targets of Infection of SARS-CoV-2 in Syrian Golden Hamsters. *Viruses* **13**, doi:10.3390/v13081653 (2021).
23. Lee, C. Y. & Lowen, A. C. Animal models for SARS-CoV-2. *Current opinion in virology* **48**, 73-81, doi:10.1016/j.coviro.2021.03.009 (2021).
24. Imai, M. *et al.* Syrian hamsters as a small animal model for SARS-CoV-2 infection and countermeasure development. *Proceedings of the National Academy of Sciences of the United States of America* **117**, 16587-16595, doi:10.1073/pnas.2009799117 (2020).
25. Yoshihara, Y. *et al.* OCAM: A new member of the neural cell adhesion molecule family related to zone-to-zone projection of olfactory and vomeronasal axons. *The Journal of neuroscience : the official journal of the Society for Neuroscience* **17**, 5830-5842 (1997).
26. Mori, K., von Campenhause, H. & Yoshihara, Y. Zonal organization of the mammalian main and accessory olfactory systems. *Philosophical transactions of the Royal Society of London. Series B, Biological sciences* **355**, 1801-1812, doi:10.1098/rstb.2000.0736 (2000).
27. Imamura, F. & Hasegawa-Ishii, S. Environmental Toxicants-Induced Immune Responses in the Olfactory Mucosa. *Frontiers in immunology* **7**, 475, doi:10.3389/fimmu.2016.00475 (2016).
28. Gussing, F. & Bohm, S. NQO1 activity in the main and the accessory olfactory systems correlates with the zonal topography of projection maps. *The European journal of neuroscience* **19**, 2511-2518, doi:10.1111/j.0953-816X.2004.03331.x (2004).
29. Furukawa, R. *et al.* Persimmon-derived tannin has antiviral effects and reduces the severity of infection and transmission of SARS-CoV-2 in a Syrian hamster model. *Scientific reports* **11**, 23695, doi:10.1038/s41598-021-03149-3 (2021).
30. Ueha, R. *et al.* Damage to Olfactory Progenitor Cells Is Involved in Cigarette Smoke-Induced Olfactory Dysfunction in Mice. *The American journal of pathology* **186**, 579-586, doi:10.1016/j.ajpath.2015.11.009 (2016).
31. Ueha, R. *et al.* Cigarette Smoke Delays Regeneration of the Olfactory Epithelium in Mice. *Neurotoxicity research* **30**, 213-224, doi:10.1007/s12640-016-9617-5 (2016).
32. Ueha, R., Ueha, S., Kondo, K., Kikuta, S. & Yamasoba, T. Cigarette Smoke-Induced Cell Death Causes Persistent Olfactory Dysfunction in Aged Mice. *Frontiers in aging neuroscience* **10**, 183, doi:10.3389/fnagi.2018.00183 (2018).
33. Ueha, R., Kondo, K., Ueha, S. & Yamasoba, T. Dose-Dependent Effects of Insulin-Like Growth Factor 1 in the Aged Olfactory Epithelium. *Frontiers in aging neuroscience* **10**, 385, doi:10.3389/fnagi.2018.00385 (2018).

34. Loria, V., Dato, I., Graziani, F. & Biasucci, L. M. Myeloperoxidase: a new biomarker of inflammation in ischemic heart disease and acute coronary syndromes. *Mediators of inflammation* **2008**, 135625, doi:10.1155/2008/135625 (2008).
35. Ueha, R. *et al.* Acute inflammatory response to contrast agent aspiration and its mechanisms in the rat lung. *The Laryngoscope* **129**, 1533-1538, doi:10.1002/lary.27663 (2019).
36. Lazarini, F., Gabellec, M. M., Torquet, N. & Lledo, P. M. Early activation of microglia triggers long-lasting impairment of adult neurogenesis in the olfactory bulb. *The Journal of neuroscience : the official journal of the Society for Neuroscience* **32**, 3652-3664, doi:10.1523/JNEUROSCI.6394-11.2012 (2012).
37. Ueha, R., Ueha, S., Kondo, K., Nishijima, H. & Yamasoba, T. Effects of Cigarette Smoke on the Nasal Respiratory and Olfactory Mucosa in Allergic Rhinitis Mice. *Frontiers in neuroscience* **14**, 126, doi:10.3389/fnins.2020.00126 (2020).
38. Tuerdi, A. *et al.* Dorsal-zone-specific reduction of sensory neuron density in the olfactory epithelium following long-term exercise or caloric restriction. *Scientific reports* **8**, 17300, doi:10.1038/s41598-018-35607-w (2018).
39. Jiao, L. *et al.* The olfactory route is a potential way for SARS-CoV-2 to invade the central nervous system of rhesus monkeys. *Signal transduction and targeted therapy* **6**, 169, doi:10.1038/s41392-021-00591-7 (2021).
40. Morbini, P. *et al.* Ultrastructural Evidence of Direct Viral Damage to the Olfactory Complex in Patients Testing Positive for SARS-CoV-2. *JAMA otolaryngology– head & neck surgery* **146**, 972-973, doi:10.1001/jamaoto.2020.2366 (2020).
41. Meinhardt, J. *et al.* Olfactory transmucosal SARS-CoV-2 invasion as a port of central nervous system entry in individuals with COVID-19. *Nature neuroscience* **24**, 168-175, doi:10.1038/s41593-020-00758-5 (2021).
42. Strauss, S. B., Lantos, J. E., Heier, L. A., Shatzkes, D. R. & Phillips, C. D. Olfactory Bulb Signal Abnormality in Patients with COVID-19 Who Present with Neurologic Symptoms. *AJNR. American journal of neuroradiology* **41**, 1882-1887, doi:10.3174/ajnr.A6751 (2020).
43. Najt, P., Richards, H. L. & Fortune, D. G. Brain imaging in patients with COVID-19: A systematic review. *Brain, behavior, & immunity - health* **16**, 100290, doi:10.1016/j.bbih.2021.100290 (2021).
44. Golden, J. W. *et al.* Human angiotensin-converting enzyme 2 transgenic mice infected with SARS-CoV-2 develop severe and fatal respiratory disease. *JCI insight* **5**, doi:10.1172/jci.insight.142032 (2020).
45. Boscolo-Rizzo, P. *et al.* Six-Month Psychophysical Evaluation of Olfactory Dysfunction in Patients with COVID-19. *Chemical senses* **46**, doi:10.1093/chemse/bjab006 (2021).
46. Kapoor, D., Verma, N., Gupta, N. & Goyal, A. Post Viral Olfactory Dysfunction After SARS-CoV-2 Infection: Anticipated Post-pandemic Clinical Challenge. *Indian journal of otolaryngology and head and neck surgery : official publication of the Association of Otolaryngologists of India*, 1-8, doi:10.1007/s12070-021-02730-6 (2021).

Figures

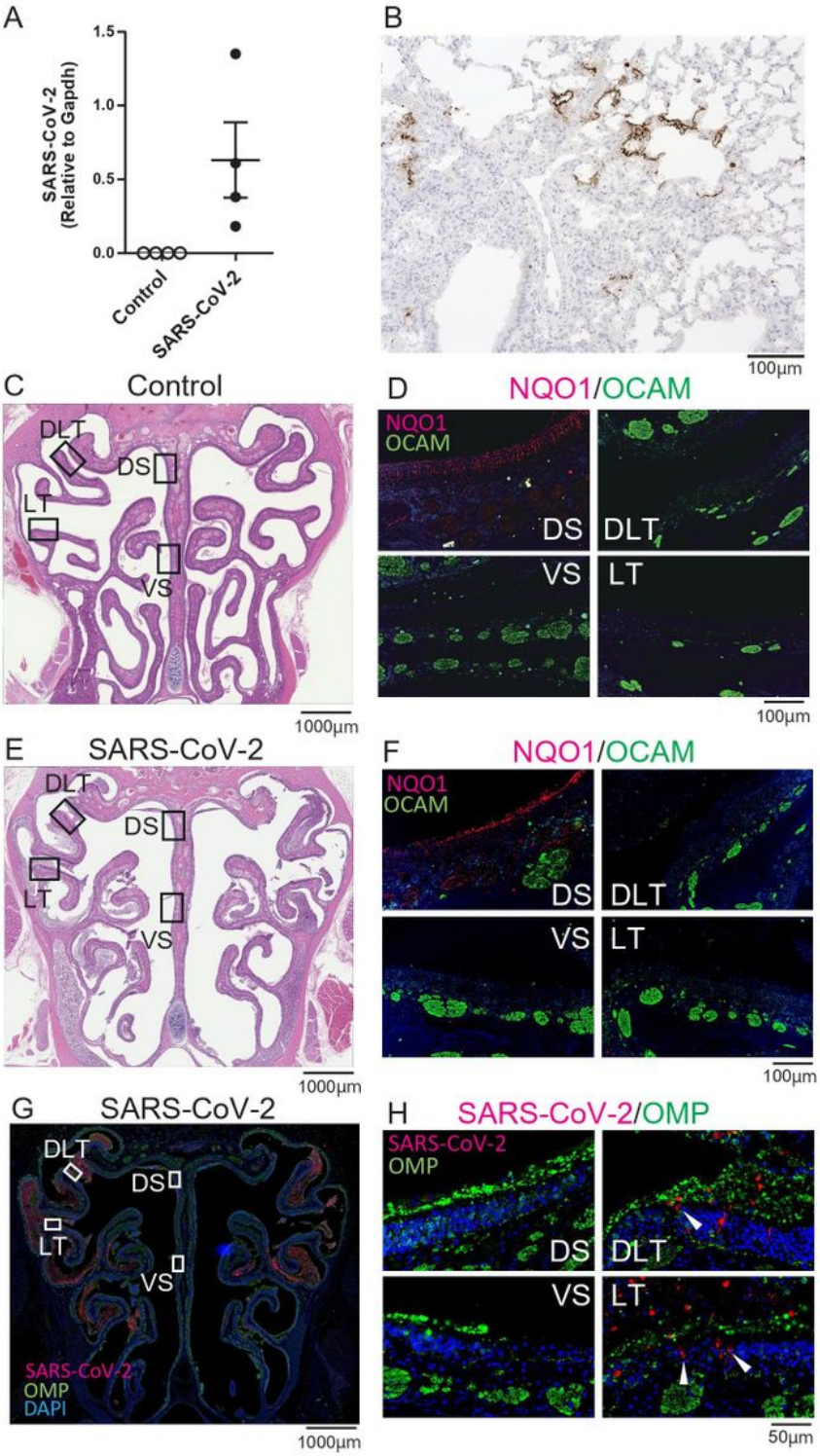

Figure 1

Infectious findings in the lungs and nasal cavity

A: Severe acute respiratory syndrome coronavirus 2 (SARS-CoV-2) gene detection with RT- quantitative polymerase chain reaction. **B**: Immunohistochemistry staining of SARS-CoV-2 (brown) in the lung. **C, D**: Representative images of the olfactory epithelium from control hamsters (C: hematoxylin and eosin stain, D: immunohistological staining of NQO1 and OCAM). The boxes in (C) indicate the regions of the olfactory epithelium shown in D; the dorsal nasal septum (DS) area, ventral nasal septum (VS) area, dorsal lateral turbinate (DLT) area, and lateral turbinate (LT) area. Only the DS area appears positive for NQO1. **E, F**: Representative images of the olfactory epithelium from SARS-CoV-2 hamsters. **G**: Immunohistochemistry staining of the olfactory epithelium in SARS-CoV-2 hamsters. The virus is mainly present in the lateral region of the nasal cavity. **H**: Double stained images of SARS-CoV-2 and OMP in each region of the olfactory epithelium. No double positive cells for SARS-CoV-2 and OMP are present in the olfactory epithelium. The arrow heads show SARS-CoV-2 positive cells.

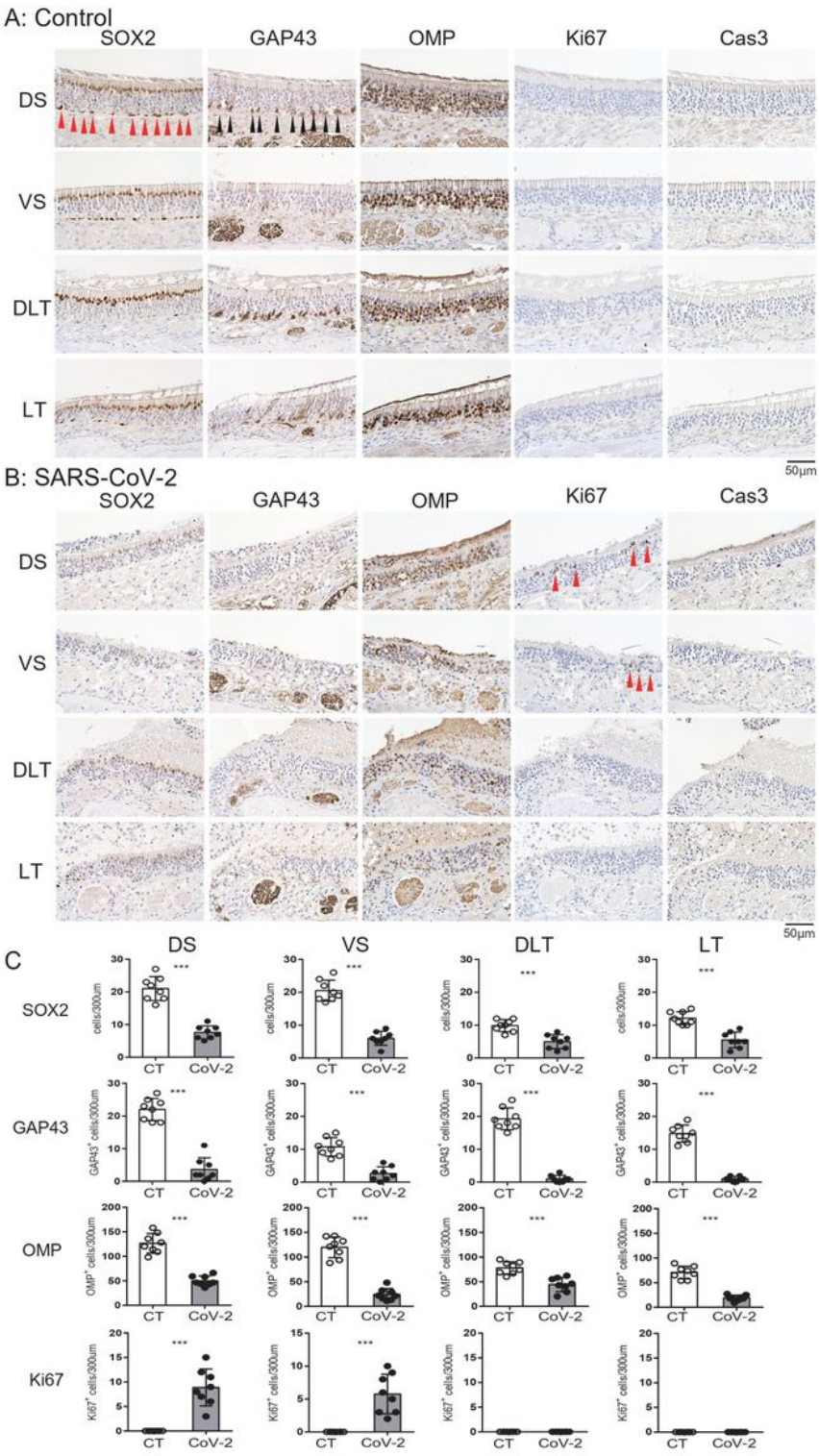

Figure 2

Effects of SARS-CoV-2 infection on the olfactory receptor neuron lineage

A, B: Representative images of immunohistological staining in control hamsters (A) and severe acute respiratory syndrome coronavirus 2 (SARS-CoV-2) hamsters (B). Sex-determining region Y-box 2 $(SOX2)^+$ progenitor cells, growth-associated protein 4 $(GAP43)^+$ immature olfactory receptor neurons (ORNs),

olfactory marker protein (OMP)$^+$ ORNs, Ki67$^+$ proliferating cells, and cleaved caspase-3 (Cas3)$^+$ apoptotic cells are shown in brown. Each cell, except for the numerous OMP+ cells, is indicated by arrows. Tissue sections were counterstained with the nuclear dye hematoxylin (blue). **C**: Numbers of SOX2$^+$ ORN progenitors and Ki67$^+$ actively proliferating cells per 300 μm of the basal layer and OMP+ mature ORNs, GAP43+ immature ORNs, and Cas3+ apoptotic cells per 300 μm of olfactory epithelium in each area are counted in control or SARS-CoV-2 hamsters. ***, P < 0.001.

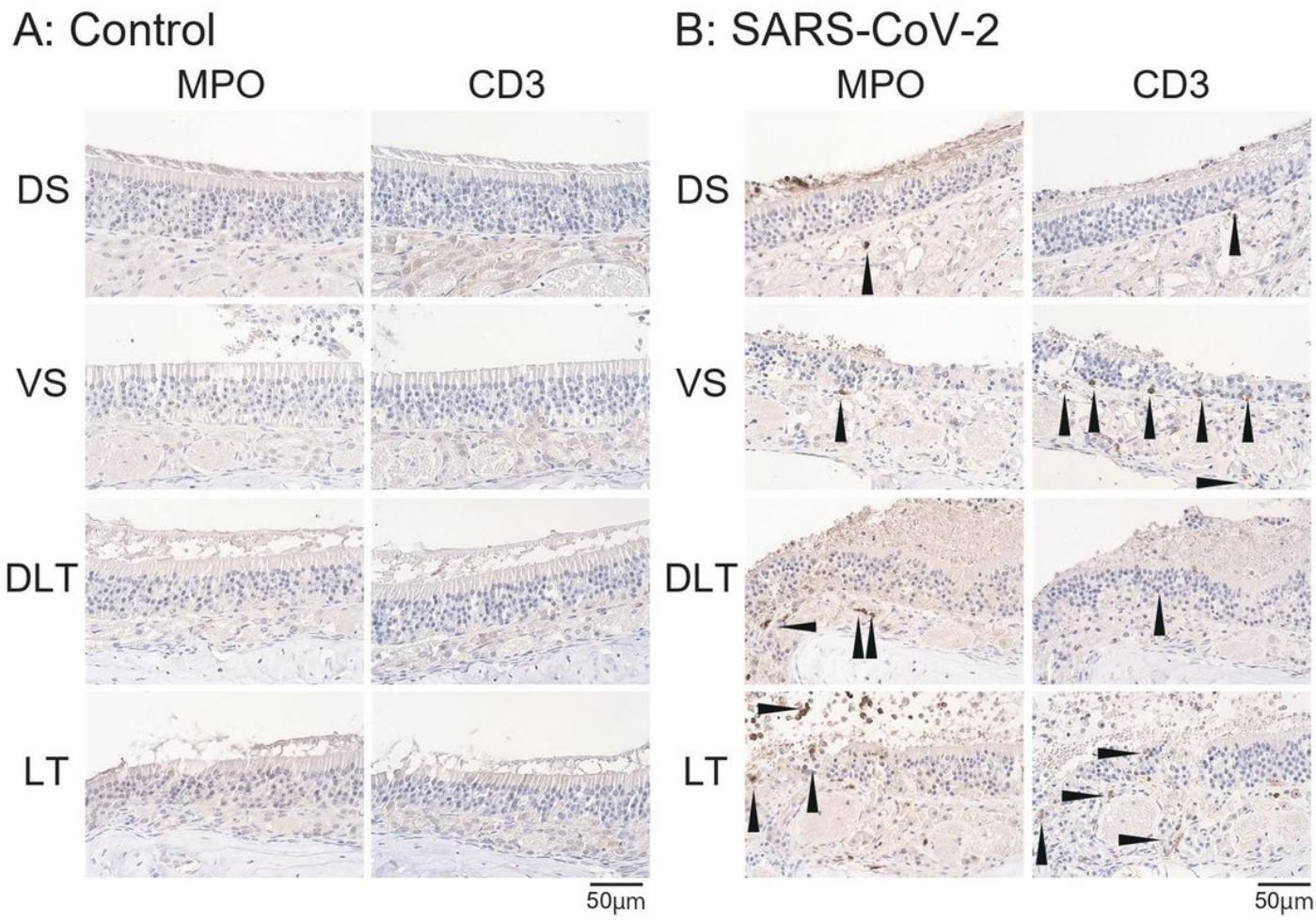

Figure 3

Inflammatory cell infiltration in the olfactory mucosa

A, B: Representative images of immunohistological staining of MPO and CD3 in control hamsters (A) and severe acute respiratory syndrome coronavirus 2 (SARS-CoV-2) hamsters (B). **B**: In the SARS-CoV-2 group, some MPO$^+$ and CD3$^+$ cells are present in the olfactory epithelium.

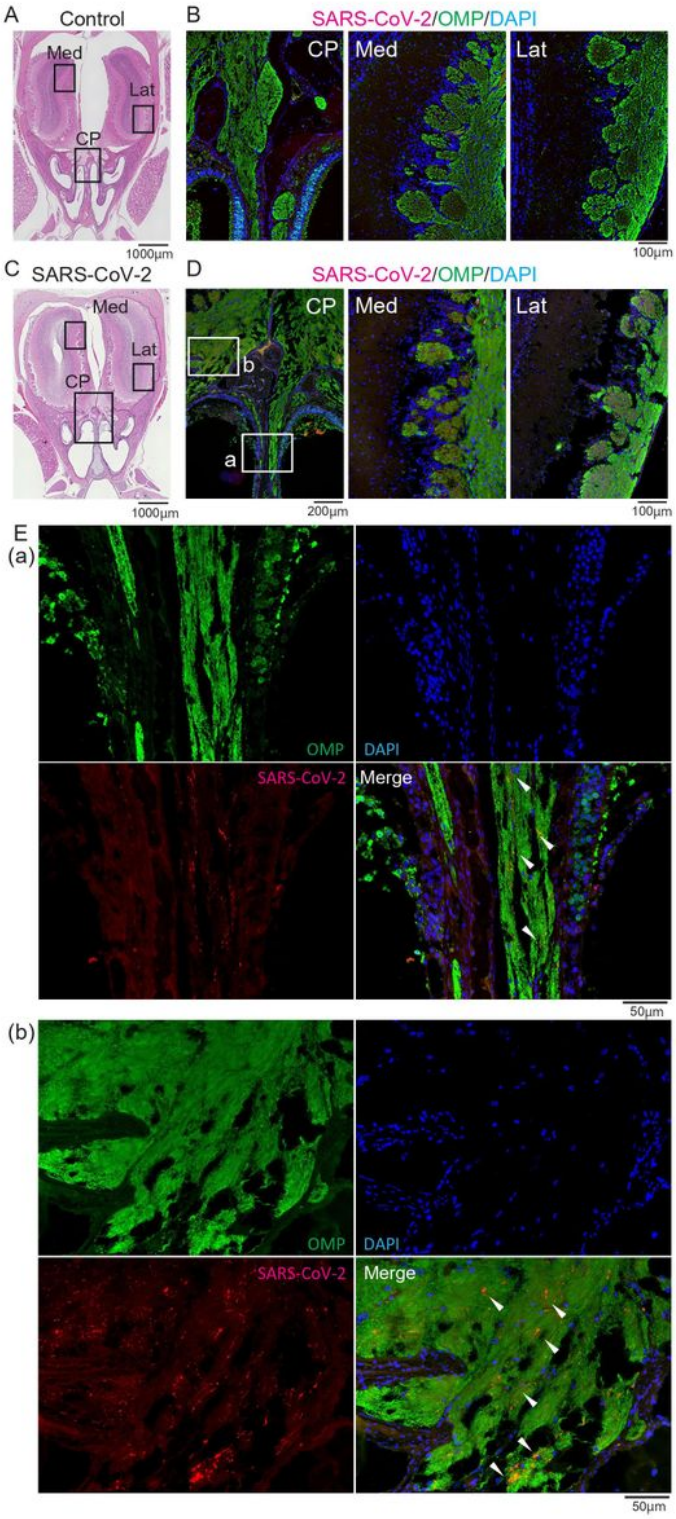

Figure 4

Representative images of SARS-CoV-2 and OMP staining in the olfactory nerve bundles and olfactory bulb

Representative coronal section images of the olfactory bulb area. **A, B**: Images of control hamsters (A: hematoxylin and eosin stain, B: immunohistological staining of severe acute respiratory syndrome

coronavirus 2 (SARS-CoV-2), olfactory marker protein (OMP), and DAPI). The boxes in (A) indicate the areas shown enlarged in B; the cribriform plate area (CP), medial area (Med), and lateral area (Lat). **C, D, E**: Images of SARS-CoV-2 hamsters (C: hematoxylin and eosin stain, D, E: immunohistological staining of SARS-CoV-2, OMP, and DAPI). The boxes in (C) indicate the areas shown enlarged in D, and the boxes in (D) are shown enlarged in (E). SARS-CoV-2 is present in the olfactory nerve of the nasal mucosa and the olfactory nerve fiber layer around the olfactory bulb.

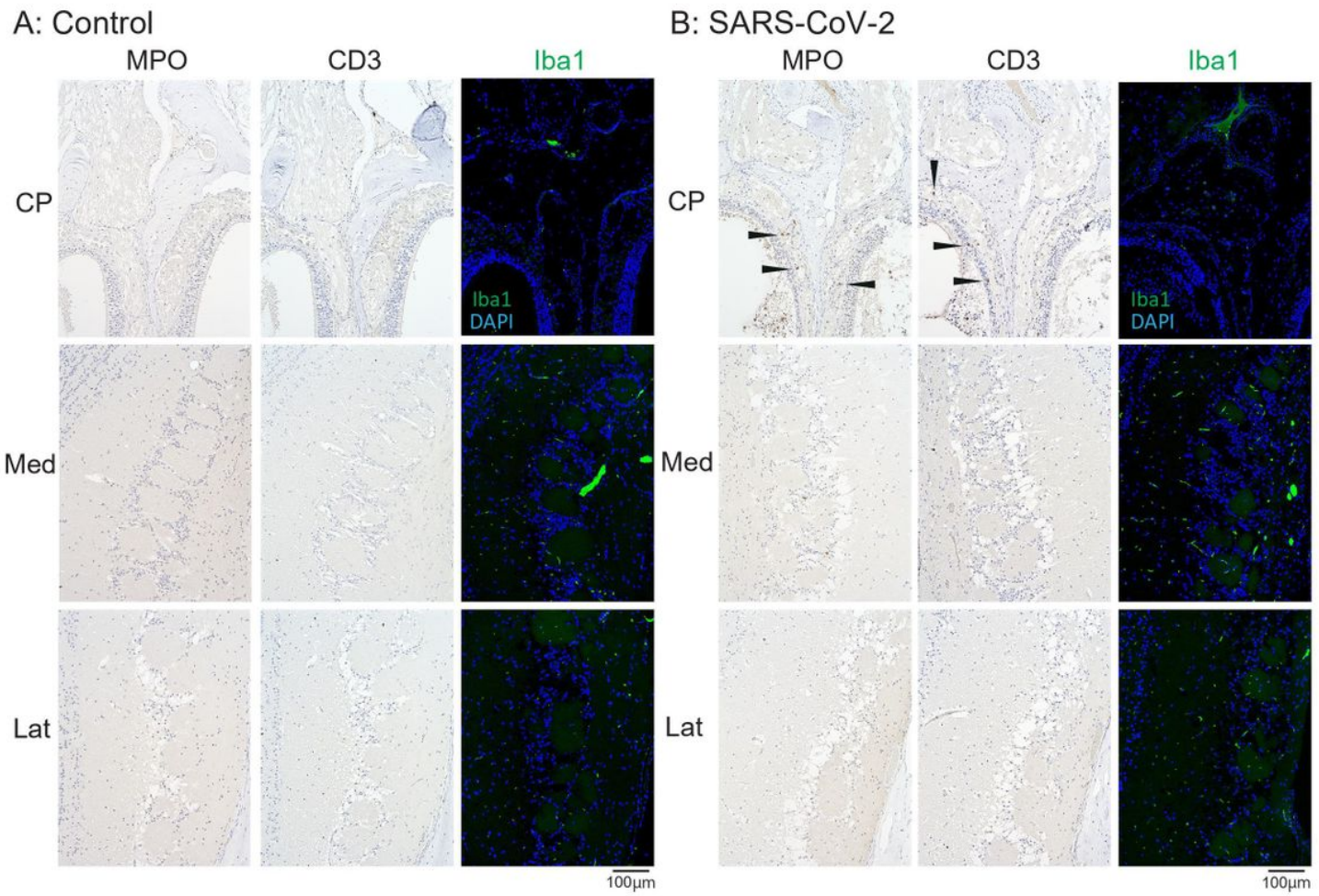

Figure 5

MPO/ CD3/ Iba1 positive cells in the olfactory bulb area

Representative immunohistological images of MPO and CD3 in the olfactory bulb area (A: control hamster, B: SARS-CoV-2 hamster). Some MPO^{+} cells and $CD3^{+}$ cells are observed in the olfactory mucosa around the cribriform plate (arrow heads).

CP: cribriform plate area, Iba1: ionized calcium-binding adaptor molecule 1, Lat: lateral area, Med: medial area, SARS-CoV-2: severe acute respiratory syndrome coronavirus 2